Thermonuclear ^{42}Ti$(p,\gamma)^{43}$V rate in type I X-ray bursts

J.J. He[1],[*] A. Parikh[2,3], B.A. Brown[4], T. Rauscher[5,6], S.Q. Hou[1,7], Y.H. Zhang[1],[†] X.H. Zhou[1], and H.S. Xu[1]

[1]*Key Laboratory of High Precision Nuclear Spectroscopy and Center for Nuclear Matter Science,*
Institute of Modern Physics, Chinese Academy of Sciences, Lanzhou 730000, China
[2]*Departament de Física i Enginyeria Nuclear, EUETIB,*
Universitat Politècnica de Catalunya, Barcelona E-08036, Spain
[3]*Institut d'Estudis Espacials de Catalunya, Barcelona E-08034, Spain*
[4]*Department of Physics and Astronomy and National Superconducting Cyclotron Laboratory,*
Michigan State University, East Lansing, Michigan 48824, USA
[5]*Centre for Astrophysics Research, School of Physics, Astronomy and Mathematics,*
University of Hertfordshire, Hatfield AL10 9AB, United Kingdom
[6]*Departement für Physik und Astronomie, Universität Basel,*
Klingelbergstrasse 82, Basel CH-4056, Switzerland
[7]*University of Chinese Academy of Sciences, Beijing 100049, China*
(Dated: March 11, 2014)

The thermonuclear rate of the ^{42}Ti$(p,\gamma)^{43}$V reaction has been reevaluated based on a recent precise proton separation energy measurement of S_p(^{43}V)=83±43 keV. The astrophysical impact of our new rates has been investigated through one-zone postprocessing type I x-ray burst calculations. It shows that the new experimental value of S_p significantly affects the yields of species between A≈40–45. As well, the precision of the recent experimental S_p value constrains these yields to better than a factor of three.

PACS numbers: 21.10.-k,21.60.Cs,26.30.+k,27.40.+z

I. INTRODUCTION

Type I X-ray bursts (XRBs) arise from thermonuclear runaways within the accreted envelopes of neutron stars in close binary systems [1, 2]. About one hundred bursting systems have been identified in the Galaxy, with light curves of about 10–100 s in duration, recurrence periods of ∼ hours to days, and peak luminosity L_{peak}≈10^4–10^5 $L_\odot$ (similar, *e.g.*, to L_{peak} of classical novae). During the thermonuclear runaway, an accreted envelope enriched in H and He may be transformed to matter strongly enriched in heavier species (up to A≈100 [3, 4]) via the αp-process and the rapid proton capture process (rp-process) [5–7]. Current XRB models do not predict the ejection of any appreciable amounts of synthesized material during the burst. Nonetheless, calculations indicate that radiative winds generated during some bursts may eject material. Studies are ongoing to examine the viability of detecting any associated absorption features. For reviews on aspects of type I X-ray bursts, see, *e.g.*, Refs. [8–10].

The rp-process is largely characterized by localized (p,γ)-(γ,p) equilibrium within particular isotonic chains near the proton drip-line. Slower β-decays (followed by fast (p,γ) reactions) connect these isotonic chains and set the timescale for processing towards heavier nuclei. In such an equilibrium situation the abundance distribution within an isotonic chain depends exponentially on nuclear mass differences as the abundance ratio between two neighboring isotones is proportional to $\exp[S_p/kT]$, where S_p is the proton separation energy and T the temperature of the stellar environment. In particular, those isotonic chains with sufficiently small S_p values (relative to XRB temperatures - at 1 GK, kT≈100 keV) need to be known with a precision of at least 50–100 keV [6, 11]. These include, among others, S_p(^{26}P), S_p(^{43}V), S_p(^{46,47}Mn), S_p(^{61}Ga), and S_p(^{65}As) [11]. As well, reliable nuclear physics input (including precise mass values and nuclear structure information) is needed for those nuclei along the rp-process path to calculate the thermonuclear reaction rates required for XRB models. Model predictions can then be compared with *e.g.*, observations of XRB light curves to extract quantitative information about the stellar environments [12].

The level structure of ^{43}V is not experimentally known. The thermonuclear rate of the ^{42}Ti$(p,\gamma)^{43}$V reaction was first estimated by Wormer *et al.* [13] based entirely on the properties of four states in the mirror nucleus ^{43}Ca [14, 15]. Later, this rate was recalculated by Herndl *et al.* [16] using two states determined through a shell model calculation of ^{43}V. Theoretical rates calculated using statistical models are available [17]; however, due to the low density of excited states expected in ^{43}V near the proton threshold, such calculations are not ideal for this reaction [18–20]. A theoretical value of S_p=90±200 keV from the atomic mass evaluation (AME85) [21] was utilized in the above rate calculations. Another theoretical value of S_p=190±230 keV was adopted in later AME95 [22] and AME03 [23] compilations.

Recently, precise mass measurements of nuclei along the rp-process path have become available. These measurements were made at the HIRFL-CSR (Cooler-Storage Ring at the Heavy Ion Research Facility in

[*]Electronic address: jianjunhe@impcas.ac.cn
[†]Electronic address: yhzhang@impcas.ac.cn

Lanzhou) [24] in an IMS (Isochronous Mass Spectrometry) mode. Masses measured include those of a series of T_z=-1/2 nuclei (^{63}Ge, ^{65}As, ^{67}Se, and ^{71}Kr) [25, 26] and T_z=-3/2 nuclei (^{41}Ti, ^{43}V, ^{45}Cr, ^{47}Mn, ^{49}Fe, ^{53}Ni, and ^{55}Cu) [27]. The proton separation energy of ^{43}V has been experimentally determined to be S_p=83±43 keV for the first time [27]. Although the predicted values in the previous compilations (AME85, AME95 and AME03) agree with the experimental value within 1 σ uncertainties, the latter is significantly more precise. This allows the uncertainty in the rate of the ^{42}Ti(p,γ)^{43}V reaction to be dramatically reduced. In this work, the thermonuclear rate of ^{42}Ti(p,γ)^{43}V has been reevaluated using the recent experimental S_p (^{43}V) value and new calculated resonant and direct capture (DC) rates. The astrophysical impact of our new rates has been investigated through one-zone postprocessing x-ray burst calculations.

II. REACTION RATE CALCULATION

A. Resonant rate

We begin by estimating the ^{42}Ti(p,γ)^{43}V resonant rate using exactly the level energies, half-lives and single-particle spectroscopic factors from the mirror nucleus ^{43}Ca [14]. A similar approach was used in Ref. [13]. The resonant rate is calculated by the well-known narrow resonance formalism [13, 16, 28],

$$N_A\langle\sigma v\rangle_{\text{res}} = 1.54 \times 10^{11}(AT_9)^{-3/2}\omega\gamma[\text{MeV}]\exp\left(-\frac{11.605E_r[\text{MeV}]}{T_9}\right)[\text{cm}^3\text{s}^{-1}\text{mol}^{-1}]. \tag{1}$$

Here, the resonant energy E_r and strength $\omega\gamma$ are in units of MeV. For the proton capture reaction, the reduced mass A is defined by $A_T/(1+A_T)$ where A_T is the target mass. The resonant strength $\omega\gamma$ is defined by

$$\omega\gamma = \frac{2J+1}{2(2J+1)}\frac{\Gamma_p \times \Gamma_\gamma}{\Gamma_{\text{tot}}}. \tag{2}$$

Here, J_T and J are the spins of the target and resonant state, respectively. Γ_p is the partial width for the entrance channel, and Γ_γ is that for the exit channel. In the excitation energy range considered in this work, other decay channels are closed [23], and hence the total width $\Gamma_{\text{tot}}\approx\Gamma_p+\Gamma_\gamma$. Similar to the approach used by Wormer et al., the gamma partial widths of the unbound states in ^{43}V were estimated by the life-times (τ) of the corresponding bound states in the mirror ^{43}Ca via $\Gamma_\gamma=\hbar/\tau$; the proton partial widths were calculated by the following equation,

$$\Gamma_p = \frac{3\hbar^2}{AR^2}P_\ell(E)C^2S_p. \tag{3}$$

Here, R=1.26×(1+42$^{\frac{1}{3}}$) fm is the nuclear channel radius [13], P_ℓ the Coulomb penetrability factor, and C^2S_p the proton spectroscopic factor of the resonance.

For this reaction, a temperature of 2 GK corresponds to a Gamow peak E_x(^{43}V)≈1.5 MeV with a width of Δ≈1.2 MeV [28]. Therefore, its resonant rate is determined by the excited states of ^{43}V up to ∼2.1 MeV. This first estimate of the resonant rate shows that the first excited state (E_x=0.373 MeV) dominates the resonant contribution below 0.2 GK, the second excited state (E_x=0.593 MeV) dominates around 0.2–1.7 GK, and the high-lying 2.067 MeV state (with much shorter life-time τ=30 fs) dominates at even higher temperature. It shows that the contribution owing to those high-lying states above 2.067 MeV is negligible at temperatures of interest in XRBs.

We then improved upon this first estimate of the resonant rate. The simplest model for calculating the isobaric-multiplet-mass-equation (IMME) is the $0f_{7/2}$ shell model used in [29] where the displacement energies in the mass region A=41-55 were used to deduce the effective isovector and isotensor two-body matrix elements. The root-mean-square difference between experiment and theory for 60 ΔZ=1 displacement energies was 12 keV. With this model the ΔZ=3 displacement energy difference between ^{43}Ca and ^{43}V (7/2$^-$) state is predicted to be 22.854(36) MeV compared to the new experimental value of 22.857(43) MeV. The agreement is impressive. In the framework of an OXBASH [30] shell model, the resonant parameters of the three states discussed above have been recalculated and summarized in Table I. These calculations are discussed in detail in Appendix A.

B. Direct capture rate

The nonresonant direct capture (DC) rate can be estimated using methods presented in Refs. [16, 28],

TABLE I: Parameters for the present ^{42}Ti$(p,\gamma)^{43}$V resonant rate calculation. The uncertainties quoted for strengths $(\omega\gamma)$ arise from the energy dependence of the widths Γ_γ and Γ_p, as well as the assumed uncertainties of spectroscopic factors (C^2S_p) (a factor of 2).

$E_x(^{43}V)$ (MeV)	E_r (MeV)^a	τ (ps)	J^π	ℓ	C^2S_p	Γ_γ (eV)	Γ_p (eV)	$\omega\gamma$ (eV)
$0.436(0.050)^b$	$0.353(0.066)$	$22(2)$	$5/2^-$	3	0.15^c	3.04×10^{-5}	5.10×10^{-9}	1.5×10^{-8} lower: 1.4×10^{-10} upper: 6.3×10^{-7}
$0.537(0.050)^b$	$0.454(0.066)$	$117(6)$	$3/2^-$	1	0.046^d	3.42×10^{-6}	6.27×10^{-5}	6.5×10^{-6} lower: 2.2×10^{-6} upper: 1.1×10^{-5}
$2.067(0.100)^b$	$1.984(0.109)$	$0.03(0.01)$	$7/2^-$	3	0.0003^e	2.19×10^{-2}	3.45×10^{-2}	5.4×10^{-2} lower: 2.2×10^{-2} upper: 1.1×10^{-1}

^{a} Resonance energies calculated using $E_r = E_x(^{43}V) - S_p^{\exp}$, where $S_p^{\exp} = 83\pm43$ keV. ^{b} Estimated theoretical uncertainties in the parenthesis. ^{c} Value from the previous (p,d) [31] and (d,t) [32] experiments. ^{d} Averaged value from the (d,p) experiments [33, 34]. ^{e} Value calculated by the OXBASH code with same model-space and interactions as in Ref.[16].

$$N_A\langle\sigma v\rangle = N_A\left(\frac{8}{\pi A}\right)^{1/2}\frac{1}{(kT)^{3/2}}\int_0^\infty S_{\rm dc}(E)\exp\left[-\frac{E}{kT}-\frac{b}{E^{1/2}}\right]dE \tag{4}$$

If $S_{\rm dc}(E)$ factor is nearly a constant over the Gamow window, the nonresonant reaction rate can be approximated in a form of [16, 28]

$$N_A\langle\sigma v\rangle_{\rm dc} = 7.83\times10^9\left(\frac{Z}{A}\right)^{1/3}T_9^{-2/3}S_{\rm dc}(E_0)[{\rm MeV\ b}]\times\exp\left[-4.249\left(\frac{Z^2A}{T_9}\right)^{1/3}\right][{\rm cm^3s^{-1}mol^{-1}}]. \tag{5}$$

The critical parameter is $S_{\rm dc}(E_0)$, the astrophysical S-factor at the Gamow energy E_0. Herndl *et al.* listed an effective $S_{\rm dc}(E_0)$ factor of 4.91×10^{-20} [MeV b] in their Table XIII. We have recalculated this factor and found that the above number is actually 4.91×10^{-2} [MeV b].

In this work, the ^{42}Ti$(p,\gamma)^{43}$V reaction rate from direct capture into ground state of ^{43}V has been calculated with a RADCAP code [35, 36] by using a Woods-Saxon nuclear potential (central + spin orbit) and a Coulomb potential of a uniform charge distribution. The nuclear potential parameters were determined by matching the bound-state energy ($E_b = 83$ keV). A spectroscopic factor of $C^2S = 0.75$ [16], which agrees with the (d,p) experimental values of 0.68 [33] and 0.55 [34], was adopted in the present calculations. The DC rate contributes to the total rate only by 10–20% in the temperature region of 2–3 GK, and dominates the rate below 0.07 GK. The RAD-

CAP calculations are described in detail in Appendix B.

C. Total reaction rate

The total reaction rate of ^{42}Ti$(p,\gamma)^{43}$V has been calculated by simply summing up the resonant and DC contributions. Our new rate is tabulated in Table II and plotted in Fig. 1. The uncertainty in the present rate arises from uncertainties in our adopted E_r (which also lead to uncertainties in the strengths since the values of Γ_p and Γ_γ have been scaled using the values of E_r - see Appendix A) and the uncertainty in the DC contribution ($\approx40\%$ - see Appendix B). In addition, we have assumed a factor of two uncertainty in the adopted spectroscopic factors. The uncertainty of the total rate is dominated by the uncertainty of the S_p value due to the
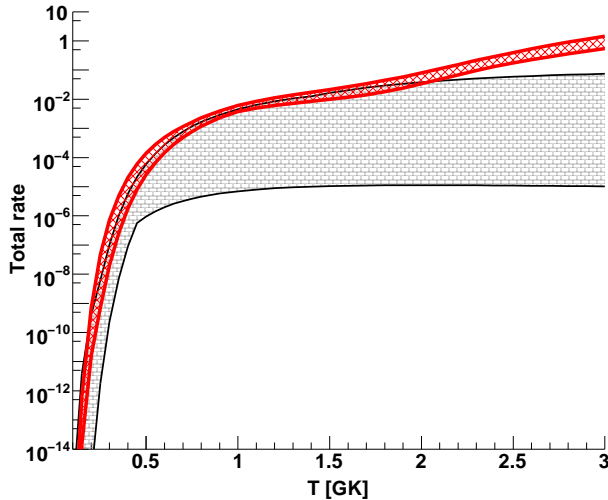
FIG. 1: (Color online) Total reaction rate calculated for the ^{42}Ti$(p,\gamma)^{43}$V reaction (in units of cm^3 mole^{-1} s^{-1}). The upper and lower limits of the present rate (with S_p=83±43 keV [27]) are shown by the (red) thicker lines, and those of the Herndl *et al.* rate (with S_p=90±200 keV [16]) are shown by the black thin lines. See text for details.

TABLE II: Reaction rates calculated for ^{42}Ti$(p,\gamma)^{43}$V. All the rates are in units of cm^3 mole^{-1} s^{-1}.

T [GK]	DC	Resonant	Total
0.01	3.69×10^{-57}	2.96×10^{-178}	3.69×10^{-57}
0.02	1.36×10^{-43}	9.44×10^{-90}	1.36×10^{-43}
0.03	5.18×10^{-37}	2.31×10^{-60}	5.18×10^{-37}
0.04	7.32×10^{-33}	1.00×10^{-45}	7.32×10^{-33}
0.05	6.56×10^{-30}	5.65×10^{-37}	6.56×10^{-30}
0.06	1.17×10^{-27}	3.66×10^{-31}	1.17×10^{-27}
0.08	2.25×10^{-24}	6.15×10^{-24}	8.40×10^{-24}
0.09	4.04×10^{-23}	1.53×10^{-21}	1.57×10^{-21}
0.10	4.87×10^{-22}	1.24×10^{-19}	1.24×10^{-19}
0.20	8.20×10^{-16}	7.58×10^{-11}	7.58×10^{-11}
0.30	8.64×10^{-13}	1.64×10^{-7}	1.64×10^{-7}
0.40	7.01×10^{-11}	8.05×10^{-6}	8.05×10^{-6}
0.50	1.60×10^{-9}	7.87×10^{-5}	7.87×10^{-5}
0.60	1.75×10^{-8}	3.44×10^{-4}	3.44×10^{-4}
0.70	1.18×10^{-7}	9.54×10^{-4}	9.54×10^{-4}
0.80	5.75×10^{-7}	2.00×10^{-3}	2.00×10^{-3}
0.90	2.19×10^{-6}	3.47×10^{-3}	3.47×10^{-3}
1.00	2.19×10^{-6}	5.32×10^{-3}	5.32×10^{-3}
1.10	1.90×10^{-5}	7.44×10^{-3}	7.46×10^{-3}
1.20	4.66×10^{-5}	9.75×10^{-3}	9.79×10^{-3}
1.30	1.04×10^{-4}	1.22×10^{-2}	1.23×10^{-2}
1.40	2.15×10^{-4}	1.48×10^{-2}	1.50×10^{-2}
1.50	4.15×10^{-4}	1.77×10^{-2}	1.81×10^{-2}
2.00	5.61×10^{-3}	5.60×10^{-2}	6.16×10^{-2}
2.50	3.65×10^{-2}	2.46×10^{-1}	2.82×10^{-1}
3.00	1.55×10^{-1}	7.90×10^{-1}	9.45×10^{-1}

exponential dependence of the rate on S_p. The rate based upon calculations in Herndl *et al.*, where only two states (at E_x=0.36, 0.55 MeV) were assumed, is also shown in Fig. 1 for comparison. Because the uncertainty of the DC contribution was not determined in Herndl *et al.*, the uncertainty of Herndl *et al.* rate shown originates only from those of the calculated resonant rates (*i.e.*, the error of S_p propagating into the strengths). It shows our new rate calculated with the precise experimental S_p value has much smaller uncertainties than the previous ones. This clearly demonstrates the importance of precise mass measurements.

Figure 2 compares five different rates for the ^{42}Ti$(p,\gamma)^{43}$V reaction: (a) present rate (Fig. 1(a)); (b) the rate from Herndl *et al.* [16]; (c) the rate from Wormer *et al.* [13]; (d) the statistical model rate ths8_v4 available in the JINA REACLIB (with S_p=-0.0189 MeV [37]); (e) the statistical model rate rath_v2 in the REACLIB [17] (with S_p=-0.411 MeV based on the FRDM mass model [38]). Because of the rather similar S_p value used, our new rate does not deviate significantly from those of Herndl *et al.* and Wormer *et al.* in the temperature region of interest in XRBs. Our new rate, however, is very well constrained with the precise mass measurement as shown in Fig. 1. The statistical-model calculations deviate from our new rate considerably over the entire temperature region of interest. This demonstrates again that the statistical-model is not ideally applicable for this reaction mainly owing to the low density of low-lying excited states in ^{43}V.

III.   ASTROPHYSICAL IMPLICATIONS

The impact of our new ^{42}Ti$(p,\gamma)^{43}$V rate was examined in the framework of one-zone XRB models. Using the representative K04 thermodynamic history (T_{peak}=1.4 GK [39]), we performed a series of postprocessing calculations to explore the role of different ^{42}Ti$(p,\gamma)^{43}$V rates and S_p values on the nuclear energy generation rate (E_{nuc}) and XRB yields. Rates of all other reactions in the network were left unchanged during these calculations. To be clear, in the discussion below we will refer explicitly to ^{42}Ti$(p,\gamma)^{43}$V forward rates (*e.g.*, as shown in Fig. 1) and to the S_p value used to determine the corresponding reverse rates through the principle of detailed balance (see, *e.g.*, [11]).

No significant differences in the respective nuclear energy generation rates were found by comparing XRB calculations with the (a) present forward rate (S_p=83 keV for the reverse rate); (b) Herndl *et al.* forward rate (S_p=88 keV); (c) Wormer *et al.* forward rate (S_p=88 keV); and (d) ths8_v4 forward rate (S_p=-19 keV). E_{nuc} determined using the rath_v2 forward rate ((e), S_p=-411 keV), however, was up to 10% lower than that from the above cases (a–d) during the burst. This (minor) dif-
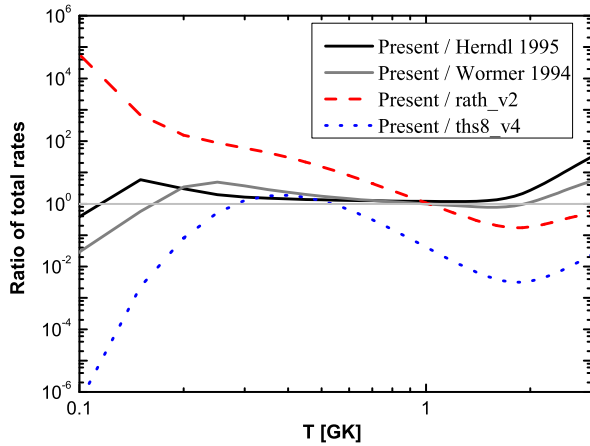
FIG. 2: (Color online) Ratios between the present rate (see Table II) and other available ones (Herndl 1995 [16], Wormer 1994 [13], rath_v2 [17] and ths8_v4 [17]).
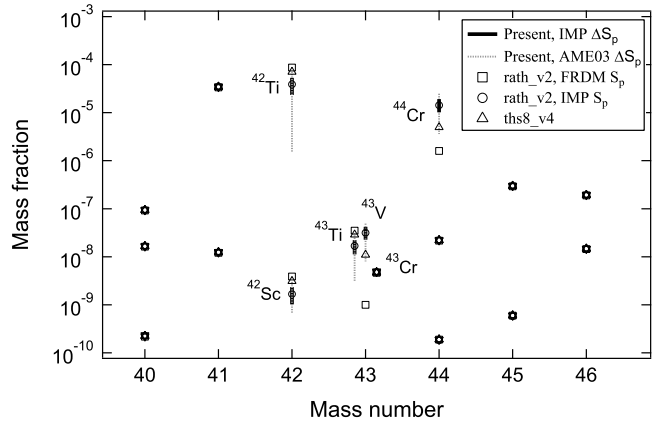

FIG. 3: Abundances following one-zone XRB calculations using the K04 thermodynamic history [39]. Abundance variations determined using the present ^{42}Ti$(p,\gamma)^{43}$V forward rate with reverse rates calculated using ΔS_p=43 keV (IMP [27], solid black line), and ΔS_p=233 keV (AME03 [23], dotted grey line) are indicated. As well, abundances determined using the rath_v2 forward rate [17] along with reverse rates calculated with S_p=-411 keV (FRDM [38], open squares) and S_p=83 keV (IMP [27], open circles) are shown. Abundances determined with the ths8_v4 rate [17] (S_p=-19 keV [37], open triangles) are also shown.

ference is attributed to the very different S_p value used in the rath_v2 reverse rate: the $E_{\rm nuc}$ from an additional XRB calculation (f) performed with a reverse rate recalculated using the rath_v2 forward rate and S_p=83 keV agreed well with the $E_{\rm nuc}$ from cases (a–d) above. This is because an equilibrium between the forward ^{42}Ti$(p,\gamma)^{43}$V and reverse ^{43}V$(\gamma,p)^{42}$Ti processes is quickly established owing to the relatively small S_p(=83 keV) of ^{43}V relative to XRB temperatures (e.g., at 1 GK, $kT\approx$100 keV). As a result, the actual rate of the ^{42}Ti$(p,\gamma)^{43}$V reaction is only of secondary importance; instead, it is the reaction Q-value (or S_p value) that characterizes the equilibrium abundances of ^{42}Ti and ^{43}V and the energy release through subsequent reactions on these species.

The effects on XRB yields by using different ^{42}Ti$(p,\gamma)^{43}$V forward rates and S_p values have been investigated. Fig. 3 shows representative yields in this mass range for the different cases discussed above, as determined immediately following the respective XRB calculations. No significant differences in yields were observed for cases (a–c,f) above. The two cases (d,e) with reverse rates determined using negative S_p values gave somewhat different yields for species with A=42–44. For example, the negative S_p values produce relatively more ^{42}Ti but less ^{43}V.

The dominant role of the S_p value used in the reverse rate in determining the yields is clearly seen in Fig. 3 from the comparison of cases (a) (labeled as "Present, IMP ΔS_p"), (d) (labeled as "ths8_v4"), (e) (labeled as "rath_v2, FRDM S_p"), and (f) (labeled as "rath_v2, IMP S_p"). It shows the yields calculated with the new experimental S_p value (for the reverse rate) significantly differ from those yields with other theoretical S_p values. In addition, to demonstrate the impact of the uncertainty in S_p, we performed additional XRB calculations using the present forward rate, along with reverse rates that reflect the one sigma uncertainties in S_p from AME03 (ΔS_p=233 keV) and the IMP mass measurement

(ΔS_p=43 keV). As shown in Fig. 3, the reduced uncertainty in S_p directly influences the possible ranges of mass fractions for the affected species. Indeed, the uncertainty from the IMP mass measurement leads to variations, by less than a factor of three, in the yields of the most produced isotopes in this mass region, such as ^{42,43}Ti, ^{42}Sc, ^{43}V and ^{43,44}Cr.

IV. SUMMARY

The thermonuclear rate of the ^{42}Ti$(p,\gamma)^{43}$V reaction has been recalculated using the recent precise proton separation energy of S_p=83±43 keV measured at the HIRFL-CSR facility in Lanzhou, China. We have also used new, updated calculations of the direct capture and resonant contributions to the rate. Our new rate deviates significantly from other rates found in the literature. We confirm that statistical model calculations are not ideally applicable for this reaction primarily because of the low density of low-lying excited states in ^{43}V. We recommend that out new rate be incorporated in future astrophysical network calculations.

The astrophysical impact of our new rate has been investigated through one-zone postprocessing Type I x-ray burst calculations. Even when using dramatically different rates, we find no significant changes to the calculated nuclear energy generation rate during a representative burst. This is because equilibrium between the forward ^{42}Ti$(p,\gamma)^{43}$V and reverse ^{43}V$(\gamma,p)^{42}$Ti processes rapidly develops at XRB temperatures. As such it is the reac-

TABLE III: Mass fractions following one-zone XRB calculations using the K04 thermodynamic history [39]. These values are plotted in Fig. 3. The first two columns give ranges of mass fractions as determined using the one sigma uncertainties for $S_p(^{43}\text{V})$ from the recent measurement and other theoretical estimates.

	Mass fraction				
Species	IMP ΔS_p [27]	AME03 ΔS_p [23]	rath_v2 (FRDM S_p [38])	rath_v2 (IMP S_p)	ths8_v4 [37]
^{42}Ti	$(2.3–5.3)\times10^{-5}$	$(1.6–75)\times10^{-6}$	8.7×10^{-5}	3.9×10^{-5}	7.1×10^{-5}
^{42}Sc	$(1.0–2.3)\times10^{-9}$	$(6.9–33)\times10^{-10}$	3.9×10^{-9}	1.7×10^{-9}	3.1×10^{-9}
^{43}Ti	$(1.1–2.2)\times10^{-8}$	$(3.2–31)\times10^{-9}$	3.5×10^{-8}	1.7×10^{-8}	2.9×10^{-8}
^{43}V	$(2.3–4.2)\times10^{-8}$	$(8.0–55)\times10^{-9}$	1.0×10^{-9}	3.2×10^{-8}	1.1×10^{-8}
^{44}Cr	$(1.0–1.9)\times10^{-5}$	$(3.6–25)\times10^{-6}$	1.6×10^{-6}	1.4×10^{-5}	5.0×10^{-6}

tion Q-value (or S_p) that mainly characterizes the equilibrium abundances of ^{42}Ti and ^{43}V. In this respect, the present $^{42}\text{Ti}(p,\gamma)^{43}\text{V}$ rate and $S_p(^{43}\text{V})$ value are sufficiently well known to determine the nuclear energy generation rate within the framework of the adopted XRB model. In addition, we find that the new experimental value of S_p affects significantly the yields of a limited number of species with A=42–44, such as $^{42,43}\text{Ti}$, ^{42}Sc, ^{43}V and $^{43,44}\text{Cr}$. The precision in S_p achieved from the IMP mass measurement restricts the variation of these yields to better than a factor of three. It demonstrates clearly the importance of precise mass measurements for those key nuclei (especially those waiting-point nuclei) along the rp-process occurring in x-ray bursts.

Appendix A: Calculation of resonant parameters

Below we summarize our calculations of the resonant parameters of the three states in ^{43}V around 0.373 MeV (Resonance 1), 0.593 MeV (Resonance 2) and 2.067 MeV (Resonance 3).

1. Resonance 1

In the $0f_{7/2}$ model, the energy of the first excited $5/2^-$ state is predicted to be 63 keV higher in ^{43}V compared to ^{43}Ca. Thus, with the experimental energy of 0.370 keV

for ^{43}Ca we obtain a predicted excitation energy of 0.436 MeV (E_r=0.353 MeV) for ^{43}V.

The $5/2^-$ to $7/2^-$ transition in ^{43}Ca has an experimental $B(M1)$ value of 0.023(2) μ_N^2. In the pf model space with the FPD6 interaction [40] the $B(M1)$ values are predicted to be 0.018, 0.025 μ_N^2 for the excited states in ^{43}Ca and ^{43}V, respectively. Therefore, a value of $B(M1)$=0.032 μ_N^2 is derived for the predicted 0.436 MeV state, and Γ_γ is thus calculated to be about 3.04×10^{-5} eV. This implies that the resonance strength for this state is determined by the much smaller Γ_p.

Wormer et al. estimated a resonant strength value of $\omega\gamma$ =1.0×10^{-10} eV for the E_r=0.28 MeV state. A spectroscopic factor of 0.014 would reproduce their proton width of $\Gamma_p \approx 3.3\times10^{-11}$ eV based on Eq. 3. Later, Herndl et al. estimated a value of Γ_p=1.1×10^{-12} eV with a spectroscopic factor of 0.008, by the equation of

$$\Gamma_p = C^2 S_p \times \Gamma_{\text{sp}}, \quad (A1)$$

where the single-particle width Γ_{sp} was calculated from the scattering phase shifts in a Woods-Saxon potential [41, 42] whose depth was determined by matching the resonant energy. Based on the method introduced in Ref. [43], we have recalculated this proton width using Equ. A1 with potential parameters of E_r=0.27 MeV, r_0=1.17 fm, a=0.69 fm and r_c=1.28 fm. The justification of the choice of the parameters can be found in [43]. We have obtained a single-particle width of Γ_{sp}=1.76×10^{-10} eV, which roughly agrees with the value of 1.38×10^{-10} eV calculated by Herndl et al.

Neutron spectroscopic factor measurements imply values of $S_n \approx 0.15$ [31, 32], in disagreement with the values assumed by Wormer et al. and Herndl et al. We assumed S_p=S_n in the following proton width calculations. With Equ. A1, a width of Γ_p=5.10×10^{-9} eV was obtained with the above parameters of r_0=1.17 fm, a=0.69 fm and r_c=1.28 fm (parameter Set 3 in Table IV). The proton width calculated by Eq. 3 is always larger than that by Eq. A1, because the former equation does not take the dimensionless single-particle reduced width θ_{sp}^2 [43] into account. θ_{sp}^2 is usually assumed to be unity, although this is not appropriate for many cases [43]. Here, θ_{sp}^2 is

calculated to be 0.24.

2. Resonance 2

A description of the $3/2^-$ excited state requires the full pf shell-model basis. With the empirically determined isospin-nonconserving interactions for the pf shell [44], the second excited $3/2^-$ state in ^{43}V is estimated to be located at E_x=0.537 MeV (E_r=0.454 MeV).

A spectroscopic factor of C^2S=0.046 averaged from the (d,p) experiments [33, 34] was used for this state, as adopted in Ref. [13]. The proton width is calculated to be 6.27×10^{-5} eV (θ_{sp}^2=0.56) with the same parameter Set 3 (Table IV). Since it is difficult to make a reliable life-time calculation for this state, we estimated this Γ_γ based on the mirror life-time. In the mirror ^{43}Ca, this state decays either to the ground state (J^π=$7/2^-$) or to the first excited state (J^π=$5/2^-$) with branching ratios [15] of 70.2% and 29.8%, respectively. The ground-state transition is a pure $E2$, whose width can be estimated by the relation of $\Gamma_\gamma(E2)=S \times \Gamma_\gamma^W(E2) \times BR$ [45]. Here, S is the strength of the transition in Wiesskopf units, and BR is the branching ratio (70.2%). The Weisskopf-unit gamma width (in eV) for an $E2$ transition is $\Gamma_\gamma^W(E2)=4.9 \times 10^{-8} A^{4/3} E_\gamma^5$ [45, 46] with A=43. This results in a ground-state-transition width of $\Gamma_\gamma(E2) \approx 1.7 \times 10^{-6}$ eV with S=7.2 [45]. The first-excited-state transition is a mixture of $M1$ and $E2$, where the dominant $M1$ width can be calculated by the relation of $\Gamma_\gamma(M1)=S \times \Gamma_\gamma^W(M1) \times BR$. Here, a value of S=7.6×10^{-3} [45] was adopted in the calculation. The Weisskopf-unit gamma width (in eV) for an $M1$ transition is $\Gamma_\gamma^W(M1)=2.1 \times 10^{-2} E_\gamma^3$ [45, 46]. $\Gamma_\gamma(M1)$ is estimated to be about 4.9×10^{-7} eV with a branching ratio of 29.8%. Therefore, only the ground-state-transition dominates the actual total Γ_γ width, and the energy dependence of Γ_γ can be accounted for by using the scale factor E_γ^5. For the 0.593-MeV state in ^{43}Ca, Γ_γ is about 5.62×10^{-6} eV (as estimated from the lifetime of 117 ps) In this work, we have adopted a value of Γ_γ=3.42×10^{-6} eV for the 0.537-MeV state in ^{43}V by correcting for the energy difference between ^{43}V (E_x=0.537 MeV) and ^{43}Ca (E_x=0.593 MeV).

3. Resonance 3

The higher-lying 2.067-MeV $7/2^-$ state in ^{43}Ca is not described in the pf model space, and requires nucleons to be excited from the sd shell for its description. We do not have a good model for its displacement energy and simply use the same value for its excitation energy in ^{43}V with an estimated error of 100 keV.

The Γ_γ for this state was calculated to be 2.19×10^{-2}

eV with a mirror life-time of τ=0.03 ps. In the mirror ^{43}Ca, this state mainly decays to the ground state (J^π=$7/2^-$) and to the first excited state (J^π=$5/2^-$) with branching ratios [15] of 78% and 22%, respectively; both γ transitions have $M1(E2)$ characters. By using the same strength S value for the above 0.537 MeV state with respect to $E2$ and $M1$ transitions, γ widths of the ground-state and first-excited transitions were calculated. It is found that the ground-state $E2$ transition dominates the total Γ_γ for this state. Therefore, the factor E_γ^5 was again used to account for the energy dependence of Γ_γ. The proton width Γ_p was calculated to be 3.45×10^{-2} eV with parameter Set 3 (Table IV). We have used a spectroscopic factor of 0.0003 as determined with the OXBASH code (using the same model-space and interactions as in Ref. [16]). This factor may be larger in nature, and should be determined experimentally.

Appendix B: Calculation of direct capture rate

The astrophysical S factor of the direct-capture ^{42}Ti$(p,\gamma)^{43}$V reaction has been calculated by the RADCAP code. The calculated S_{dc} factors are shown in Fig. 4 with three parameter sets listed in Table IV. With a spin-orbit potential of V_{so}=-10 MeV, the $S_{dc}(E)$ factors calculated using three sets of parameters (Table IV) vary by no more than 15% over the energy range of 0–3 MeV. This energy range covers the Gamow window for a temperature up to 3 GK. The above changes can not be regarded as substantial. Since Huang et $al.$ [36] reproduced successfully the S factors for a series of radiative capture reactions, we have adopted their potential parameters (Set 1 in Table IV) in the final DC rate calculation. The present S_{dc} factors can be well parameterized in a Taylor-series form [28] of $S_{dc}(E)=\sum_{k=1}^{k} \frac{S^{(k)}(0)}{k!} E^k$, where S factors are in units of [MeV b] and E in MeV. The fitted parameters are $S(0)$=3.97×10^{-2} [MeV b] for the S factor at zero energy, and the derivatives with respect to energy are $S^{(1)}(0)$=3.37×10^{-2}, $S^{(2)}(0)$=1.31×10^{-2}, $S^{(3)}(0)$=9.72×10^{-3} and $S^{(4)}(0)$=1.18×10^{-2}, respectively.

In addition, the parameter dependence on $S_{dc}(E)$ has been studied and the results are shown in Fig. 5. It shows that S_{dc} factor is insensitive to the parameters V_{so} and R_c (or r_c), but rather sensitive to the parameters R_0 (or r_0) and a. The choice of parameter ranges is based on the literature values [43, 47, 48]. The error of the present DC rate is estimated simply by adding in quadrature the uncertainties originating from the potential parameters discussed above; it is about ~40% in the energy range of 0–3 MeV. The DC rate as a function of temperature is calculated by numerical integration of our calculated S factors using an EXP2RATE code [49].

TABLE IV: Potential parameter lists used in the $S_{\rm dc}$ factor calculations.

Parameters	Set 1 [36]	Set 2 [47]^b	Set 3 [43]^b
$R_0=R_{so}$ (fm)^a	$1.25\times(1+42)^{\frac{1}{3}}$ [$r_0=r_{so}$=1.26]	$1.25\times42^{\frac{1}{3}}$ [$r_0=r_{so}$=1.25]	$1.25\times42^{\frac{1}{3}}$-0.23 [=$1.17\times42^{\frac{1}{3}}$, $r_0=r_{so}$=1.17]
R_c (fm)^a	$1.25\times(1+42)^{\frac{1}{3}}$ [r_c=1.26]	$1.25\times42^{\frac{1}{3}}$ [r_c=1.25]	$1.24\times42^{\frac{1}{3}}$+0.12 [=$1.28\times42^{\frac{1}{3}}$, r_c=1.28]
$a_0=a_{so}$ (fm)	0.65	0.65	0.69
V_{so} (MeV)	-10.0	-10.0	-10.0
V_0 (MeV)^c	-100.48	-101.73	-111.22
$S_{\rm dc}(0)$ (MeV b)	3.98×10^{-2}	3.84×10^{-2}	3.48×10^{-2}

^{a} r_0, r_{so} and r_c are commonly defined as $r=R/A^{\frac{1}{3}}$ for comparison. ^{b} The choice of parameters can be found in Ref. [43]. ^{c} V_0 is varied to match the bound-state energy E_b=83 keV.
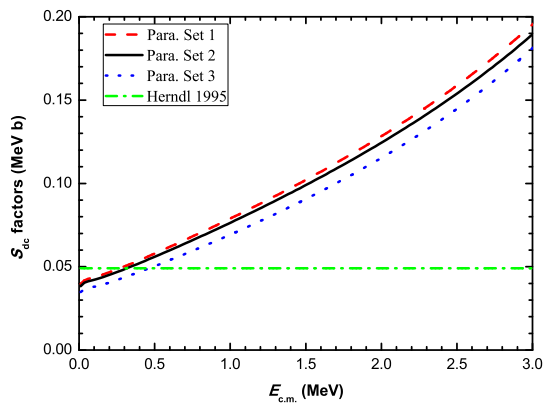

FIG. 4: (Color online) Direct-capture $S_{\rm dc}$ factors calculated with three parameter sets listed in Table IV. A previous constant value of $S_{\rm dc}(E_0)$=4.91×10^{-2} [MeV b] (Herndl 1995 [16]) is shown for comparison.

[1] S.E. Woosley and R.E. Taam, Nature **263**, 101 (1976).
[2] P.C. Joss, Nature **270**, 310 (1977).
[3] H. Schatz *et al.*, Phys. Rev. Lett. **86**, 3471 (2001).
[4] V.-V. Elomaa *et al.*, Phys. Rev. Lett. **102**, 252501 (2009).
[5] R.K. Wallace and S.E. Woosley, Astrophys. J. Suppl. **45**, 389 (1981).
[6] H. Schatz *et al.*, Phys. Rep. **294**, 167 (1998).
[7] S.E. Woosley *et al.*, Astrophys. J. Suppl. **151**, 75 (2004).
[8] W. Lewin *et al.*, Space Sci. Rev. **62**, 223 (1993).
[9] T. Strohmayer, L. Bildsten, in: W. Lewin, M. van der Klis (Eds.), Compact Stellar X-Ray Sources, (Cambridge Univ. Press, Cambridge, 2006).
[10] A. Parikh *et al.*, Prog. Part. Nucl. Phys. **69**, 225 (2013).
[11] A. Parikh *et al.*, Phys. Rev. C **79**, 045802 (2009).
[12] H. Schatz and K. E. Rehm, Nucl. Phys. **A777**, 601 (2006).
[13] L. Van Wormer *et al.*, Astrophy. J. **432**, 326 (1994).
[14] P.M. Endt and C. Van Der Leun, Nucl. Phys. **A310**, 1 (1978).
[15] P.M. Endt, Nucl. Phys. **A521**, 1 (1990).
[16] H. Herndl *et al.*, Phys. Rev. C **52**, 1078 (1995).

[17] JINA Reaclib Database, please see, https://groups.nscl.msu.edu/jina/reaclib/db/.
[18] T. Rauscher *et al.*, Phys. Rev. C **56**, 1613 (1997).
[19] T. Rauscher and F.-K. Thielemann, At. Data Nucl. Data Tables **75**, 1 (2000).
[20] T. Rauscher and F.-K. Thielemann, At. Data Nucl. Data Tables **79**, 47 (2001).
[21] G. Audi and A.H. Wapstra, Nucl. Phys. **A432**, 1 (1985).
[22] G. Audi and A.H. Wapstra, Nucl. Phys. **A595**, 409 (1995).
[23] G. Audi *et al.*, Nucl. Phys. **A729**, 337 (2003).
[24] J. W. Xia *et al.*, Nucl. Instr. Meth. **A 488**, 11 (2002).
[25] X.L. Tu *et al.*, Phys. Rev. Lett. **106**, 112501 (2011).
[26] Y.H. Zhang *et al.*, Phys. Rev. Lett. **109**, 102501 (2012).
[27] X.L. Yan *et al.*, Astrophy. J. Lett. **766**, L8 (2013).
[28] C.E. Rolfs and W.S. Rodney, *Cauldrons in the Cosmos*, (University of Chicago Press, Chicago, 1988)
[29] B.A. Brown and R. Sherr, Nucl. Phys. **A322**, 61 (1979).
[30] B.A. Brown, E. Etchegoyen, W.D.M. Rae, and N.S. Godwin, OXBASH, 1984 (unpublished).
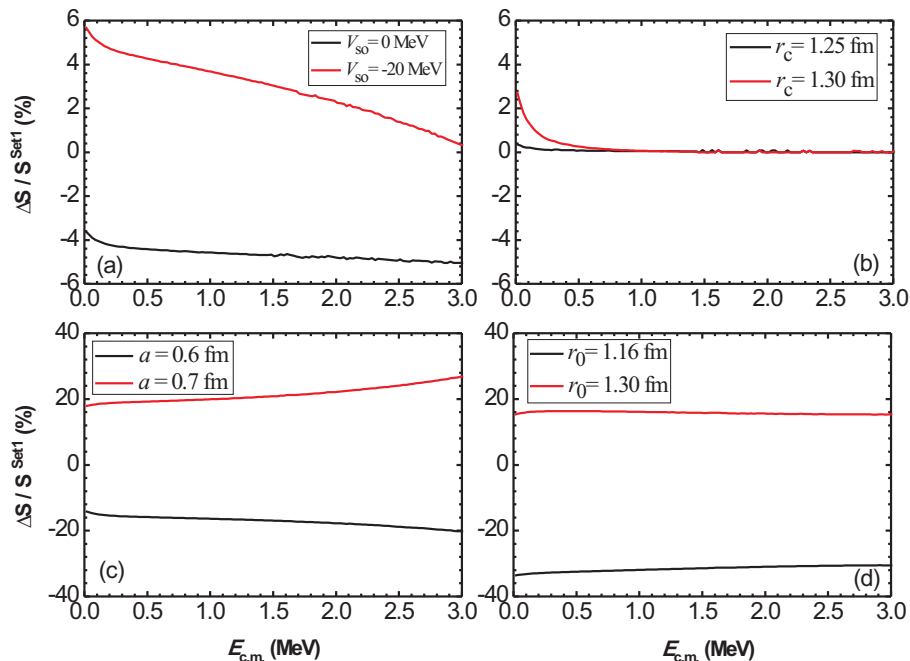[31] S.M. Smith *et al.*, Nucl. Phys. **A113**, 303 (1968).

FIG. 5: (Color online) Dependence of S_{dc} factors on parameters (a) spin-orbit potential V_{so}, (b) Coulomb radius parameter r_c, (c) diffuseness a, and (d) optical-model (real) potential radius parameter r_0. Here, radius r is defined as $r=R/A^{\frac{1}{3}}$, with $r_0=r_{so}$, $a_0=a_{so}$ in all calculations.

[32] P. Doll *et al.*, Nucl. Phys. **A263**, 210 (1976).
[33] W.E. Dorenbusch, T.A. Belote, and O. Hansen, Phys. Rev **146**, 734 (1966).
[34] G. Brown, A. Denning, J.G.B. Haigh, Nucl. Phys. **A225**, 267 (1974).
[35] C.A. Bertulani, Comput. Phys. Commun. **156**, 123 (2003).
[36] J.T. Huang *et al.*, Atom. Data Nucl. Data Tables **96**, 824 (2010).
[37] R.H. Cyburt *et al.*, Astrophys. J. Suppl. **189**, 240 (2010).
[38] P. Möller *et al.*, Atom. Data Nucl. Data Tables **59**, 185 (1995).
[39] A. Parikh *et al.*, Astrophys. J. Suppl. **178**, 110 (2008).
[40] W.A. Richter, M.G. van der Merwe, R.E. Julies, and B.A. Brown, Nucl. Phys. **A523**, 325 (1991).
[41] B.A. Brown *et al.*, Phys. Rev. C **48**, 1456 (1993).
[42] A.E. Champagne *et al.*, Nucl. Phys. **A556**, 123 (1993).
[43] C. Iliadis, Nucl. Phys. **A618**, 166 (1997).
[44] W.E. Ormand and B.A. Brown, Nucl. Phys. **A491**, 1 (1989).
[45] P.M. Endt, Atom. Data Nucl. Data Tables **23**, 3 (1979).
[46] D.H. Wilkinson, in *Nuclear Spectroscopy*, edited by F. Ajzenberg-Selove (Academic Press, New York, 1960), Vol. B.
[47] F. G. Perey, Phys. Rev. **131**, 745 (1963).
[48] R.L. Varner *et al.*, Phys. Rep. **201**, 57 (1991).
[49] T. Rauscher, *EXP2RATE v2.1*, http://nucastro.org/codes.html.